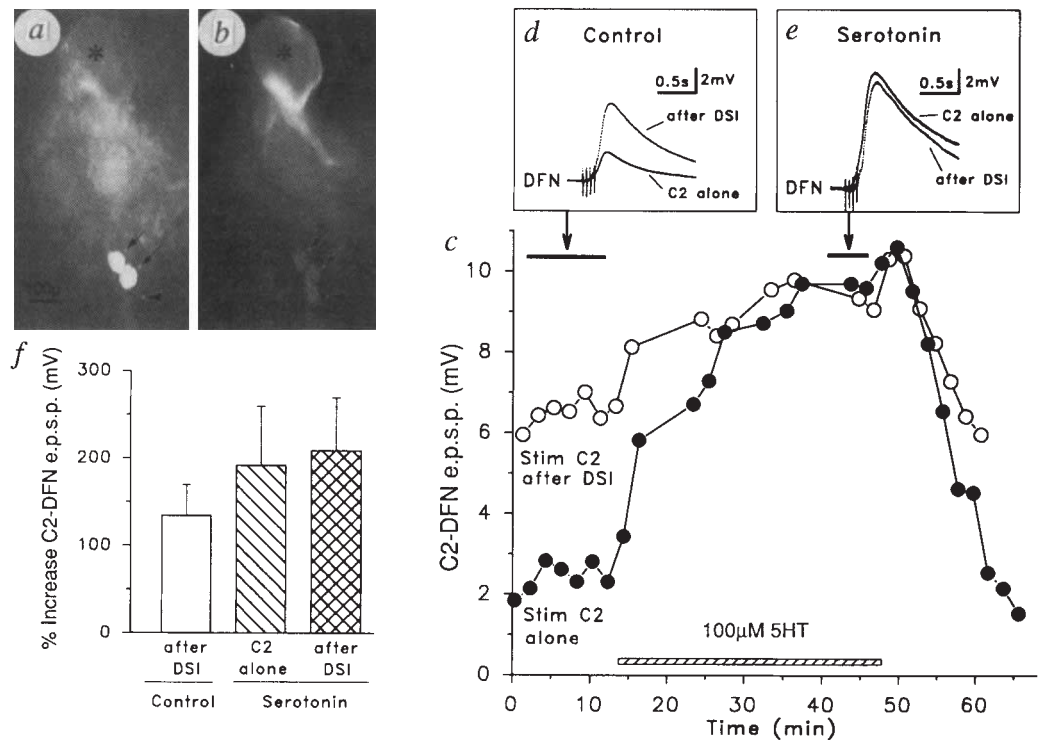


FIG. 3 Serotonin may mediate the modulatory actions of DSI. *a* and *b*, DSIs are immunoreactive for serotonin. *a*, All three ipsilateral DSI neurons were identified physiologically and two were injected with Lucifer yellow (arrows). *b*, The uninjected neuron (arrowhead) and both of the injected neurons (arrows) were recognized by an antibody against serotonin (Incstar, Stillwater, MN), visualized with a secondary antibody tagged with Texas red (Vector Lab). The giant serotonergic cerebral cell C1 (asterisk) displayed serotonin immunoreactivity as expected²⁹. Fixation and antibody procedures were modified from ref. 30. *c*, Serotonin mimics and occludes the modulatory effects of DSI. Brief C2 trains (4 pulses, 20 Hz) were elicited every 60 s to evoke a test e.p.s.p. in DFN; alternate C2 trains were preceded by a DSI train (5 Hz for 10 s; ending 4 s before the C2 train) to induce modulation. In control saline, the C2-DFN e.p.s.p. after DSI stimulation (open circles) was larger than the e.p.s.p. evoked when C2 was stimulated alone (filled circles). Switching the bath solution to 100 μ M serotonin (hatched bar) caused the C2-evoked e.p.s.ps to increase in amplitude, mimicking the effect of DSI stimulation. After 30 min, the e.p.s.p. enhancement caused by serotonin was maximal and the modulatory effect of DSI was occluded. Upon switching back to control saline, the C2-evoked e.p.s.p. returned to its original amplitude and the modulatory actions of DSI reappeared. *d* and *e*, Excerpts from the experiment in *c*, showing averaged compound C2-DFN e.p.s.ps, evoked by C2 stimulation alone and after DSI stimulation, which were taken from the periods



indicated by the black bars, in control saline (*d*) and 100 μ M serotonin (*e*). *f*, Average data from three experiments. DSI produced a 134% enhancement of the C2-DFN e.p.s.p. in control saline. Serotonin mimicked this effect, producing a 191% increase in the C2-DFN e.p.s.p. In serotonin, the ability of DSI to produce further enhancement of the e.p.s.p. was occluded (208% total enhancement). All experiments were done in high-divalent-ion saline and in each case DFN was impaled with two electrodes for independent voltage recording and current injection. The resting potential was held at -70 mV by injecting current into the DFN, countering the direct depolarizing action of serotonin.

Received 22 October; accepted 1 December 1993.

- Harris-Warrick, R. M. & Marder, E. A. *Rev. Neurosci.* **14**, 39–57 (1991).
- Kaczmarek, L. K. & Levitan, I. B. *Neuromodulation: The Biochemical Control of Neuronal Excitability* (Oxford Univ. Press, New York, 1987).
- Gettings, P. A., Lennard, P. R. & Hume, R. I. *J. Neurophysiol.* **44**, 151–164 (1980).
- Gettings, P. A., McClellan, A. D. & Li, M. *Soc. Neurosci. Abstr.* **11**, 1023 (1985).
- Gettings, P. A. & Dekin, M. S. in *Model Neural Networks and Behavior* (ed. Selverston, A. I.) 3–20 (Plenum, New York, 1985).
- Frost, W. N. & Gettings, P. A. *Soc. Neurosci. Abstr.* **15**, 1118 (1989).
- Gettings, P. A. *J. Neurophysiol.* **46**, 65–79 (1981).
- Katz, P. S. & Frost, W. N. *Soc. Neurosci. Abstr.* **19**, 1700 (1993).
- Gettings, P. A. in *Symposia of the Society for Experimental Biology No. 37: Neural Origin of Rhythmic Movements* (eds Roberts, A. & Roberts, B. L.) 89–128 (Cambridge Univ. Press, New York, 1983).
- Gettings, P. A. & Dekin, M. S. *J. Neurophysiol.* **53**, 466–480 (1985).
- Gettings, P. A. *Rev. Neurosci.* **12**, 185–204 (1989).
- Abraham, F. D. & Willows, A. O. D. *Comm. Behav. Biol.* **6**, 271–280 (1971).
- Frost, W. N., Brown, G. & Gettings, P. A. *Soc. Neurosci. Abstr.* **14**, 607 (1988).
- Katz, P. S. & Harris-Warrick, R. M. *Trends Neurosci.* **13**, 367–373 (1990).
- Harris-Warrick, R. M. in *Neural Control of Rhythmic Movements in Vertebrates* (eds Cohen, A. H., Rossignol, S. & Grillner, S.) 285–331 (Wiley, New York, 1988).
- Jordan, L. M., Brownstone, R. M. & Noga, B. R. *Curr. Opin. Neurobiol.* **2**, 794–801 (1992).
- Hawkins, R. D., Castellucci, V. F. & Kandel, E. R. *J. Neurophysiol.* **45**, 315–326 (1981).
- Cropper, E. C. et al. *Proc. natn. Acad. Sci. U.S.A.* **84**, 3486–3490 (1987).
- Whim, M. D. & Lloyd, P. E. *J. Neurosci.* **10**, 3313–3322 (1990).
- Bishop, C. A., Wine, J. J., Nagy, F. & O'Shea, M. R. *J. Neurosci.* **7**, 1769–1779 (1987).
- Katz, P. S. & Harris-Warrick, R. M. *J. Neurophysiol.* **62**, 571–581 (1989).
- Chiel, H. J., Weiss, K. R. & Kupfermann, I. *Trends Neurosci.* **13**, 223–227 (1990).
- Nusbaum, M. P., Weimann, J. M., Golowasch, J. & Marder, E. *J. Neurosci.* **12**, 2706–2714 (1992).
- Taghert, P. H. & Willows, A. O. D. *J. comp. Physiol.* **123**, 253–259 (1978).
- Willows, A. O. D., Dorsett, D. A. & Hoyle, G. *J. Neurobiol.* **4**(3), 207–237 (1973).
- Hume, R. I., Gettings, P. A. & Del Beccaro, M. A. *J. Neurophysiol.* **47**, 60–74 (1982).
- Hume, R. I., Gettings, P. A. *J. Neurophysiol.* **47**, 75–90 (1982).
- Brown, G. D. & Willows, A. O. D. *Soc. Neurosci. Abstr.* **17**, 549 (1991).
- Weinreich, D., McCaman, M. W., McCaman, R. E. & Vaughn, J. E. *J. Neurochem.* **20**, 969–976 (1973).
- Croll, R. P. & Chiasson, B. J. *J. comp. Neurol.* **280**, 122–142 (1989).

ACKNOWLEDGEMENTS. We thank L. Eliot and S. Pallas for helpful criticism. Some of this work was conducted at Friday Harbor Laboratories, University of Washington. The work was supported by grants from the NIH and NIMH to P.S.K., P.A.G. and W.N.F.

The 'blue-on' opponent pathway in primate retina originates from a distinct bistratified ganglion cell type

Dennis M. Dacey* & Barry B. Lee†

* Department of Biological Structure, University of Washington, Seattle, Washington 98195, USA

† Max Planck Institute for Biophysical Chemistry, 37077 Göttingen, Germany

COLOUR vision in humans and Old World monkeys begins with the differential activation of three types of cone photoreceptor which are maximally sensitive to short (S), medium (M) and long (L) wavelengths. Signals from the three cone types are relayed to the retinal ganglion cells via cone-specific bipolar cell types^{1–4}. Colour-coding ganglion cells fall into two major physiological classes: the red-green opponent cells, which receive antagonistic input from M- and L-sensitive cones, and the blue-yellow opponent cells, which receive input from S-sensitive cones, opposed by combined M- and L-cone input. The neural mechanisms producing colour opponency are not understood. It has been assumed that both kinds of opponent signals are transmitted to the lateral geniculate nucleus by one type of ganglion cell, the midget cell^{5,6}. We now report that a distinct non-midget ganglion cell type, the small bistratified cell, corresponds to the physiological type that receives

excitatory input from S cones, the 'blue-on' cell. Our results thus demonstrate an anatomically distinct pathway that conveys S-cone signals to the brain. The morphology of the blue-on cell also suggests a novel hypothesis for the retinal circuitry underlying the blue–yellow opponent response.

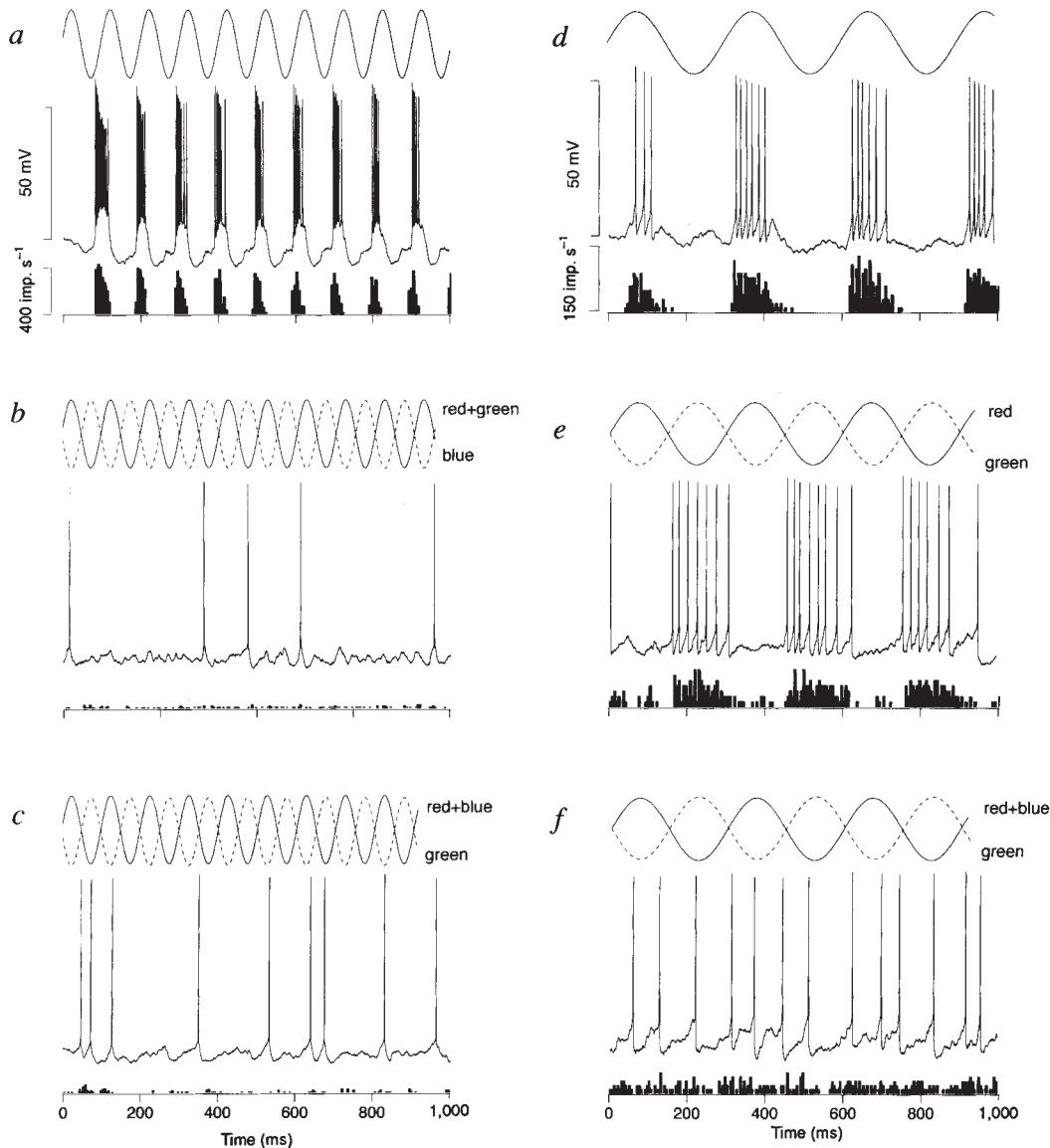
Blue-on cells were identified physiologically by intracellular recording in an *in vitro* preparation of the macaque retina. Dur-

ing recording, tracer was injected into the cell so that its morphology could be determined. Because previous intracellular studies in primates on the intact eye^{7,8} or isolated eye cup^{7,9} have been only partially successful, we used a different approach. We isolated the retina, together with the pigment epithelium and choroid, and mounted this preparation flat in a recording chamber. Complete removal of the vitreous promoted survival

FIG. 1 Intracellular responses (impulses (imp.) per s) of morphologically identified parasol and midget ganglion cells of *Macaca nemestrina* in an isolated retina–choroid preparation. *a*, Strong visual response of a cell, identified morphologically as an outer parasol cell, to the output of red and green light-emitting diodes (LEDs) modulated in phase at 10 Hz. The cell gave a phasic off-response and hyperpolarized in response to luminance increment. Top trace, stimulus composition (modulation contrast is 100% in all figures); middle trace, intracellular record; bottom, a peristimulus time histogram averaged over 20 stimulus presentations. *b*, When the output of the blue diode was adjusted to equal luminance and modulated 180° out of phase with modulation of the red and green diodes in phase (blue/yellow chromatic flicker), no response was elicited from the cell. *c*, Similarly, stimuli modulated along a tritanopic confusion line, where only S cones are modulated, evoked no response. *d–f*, Visual response of a cell identified morphologically as an inner midget cell. Luminance modulation at 3.3 Hz elicited an on-response (*d*); chromatic modulation between red and green elicited a green-on, red-off response (*e*). No midget cells gave any modulated response to the S-cone isolating stimulus (*f*).

METHODS. Eyes (*M. nemestrina*, *Macaca fascicularis* or *Macaca mulatta*) were obtained from the tissue programme of the Washington Regional Primate Research Center. The retinæ were prepared by draining the vitreous from the eye cup and dissecting the retina, pigment epithelium and choroid intact in oxygenated Ames medium. The retina–choroid was mounted in a superfusion chamber on the stage of a light microscope and kept at 36 ± 1 °C. Ganglion cell bodies were visualized by epifluorescence after staining with acridine orange. Intracellular penetrations were made under direct microscopic control and cells were recorded in conventional current clamp mode. Red, green and blue LEDs were used to deliver chromatic stimuli via a small optical bench mounted on the camera port of the microscope. Output of the LEDs was sinusoidally modulated¹¹. The red, green and blue LEDs have dominant wavelengths of about 638, 554 and 470 nm, respectively. The irradiance in the plane of the retina was measured using a Gamma Scientific spectral radiometer. We estimated retinal illuminance in these experiments to have been ~100 trolands. To produce the S-cone isolating

stimulus, human observers used flicker photometry to estimate the relative luminances of the red, green and blue diodes on white paper set on the microscope stage in the plane of the retina. These relative troland values were then corrected for the absence of macular pigmentation (all recordings were done in retinal periphery), lens and ocular media²⁶. The relative intensities predicted for an S-cone isolating stimulus were then calculated from the cone fundamentals²⁷, checked and adjusted as described elsewhere (T. Yeh, B.B.L. and J. Kremers, manuscript in preparation). Our measurements showed the retinæ to be in good physiological condition. MC cells responded down to 1–2% luminance contrast, and the S-cone cells to 5–10% S-cone modulation. These are comparable to sensitivities found *in vivo*. Also, MC-cell flicker photometric spectral sensitivities were close to the prediction, indicating that cone weightings had not been disturbed during dissection of the retina. The dendritic morphology of the recorded cells was visualized initially through the microscope by intracellular injection of the fluorescent dye pyranine during recording, and preserved for later analysis by injection of Neurobiotin (Vector; Burlingame, CA) and subsequent horseradish peroxidase histochemistry²⁸.



of the retina and we commonly obtained vigorous light responses for many hours. A crucial advantage of the *in vitro* preparation was that the retina was mounted on the stage of a light microscope so that we were able to target identified ganglion cell types visually for recording¹⁰. Retinae were vitally stained with a fluorescent dye, acridine orange, which clearly revealed the cell bodies of the two major ganglion cell classes, the large-bodied parasol cells and the small-bodied midget cells, whose axons project to the magnocellular (MC) and parvocellular (PC) layers of the lateral geniculate nucleus (LGN), respectively. Light stimuli, delivered as sinusoidal flicker from red, green and blue light-emitting diodes¹¹, were projected onto the retinal surface via the camera port of the microscope. Episcopic illumination was required to visualize and penetrate individual cell bodies, but this did not appreciably bleach the cone photopigments, as vigorous light responses could be recorded immediately after cell penetration.

We first recorded intracellularly from the two major ganglion cell classes whose axons project to the LGN, and investigated whether these cells showed any evidence of S-cone input. Morphologically identified parasol cells ($n=25$) corresponded, as predicted from previous results^{5,6}, to phasic, non-opponent cells (MC cells). As expected¹², parasol cells whose dendrites stratified in the inner portion of the inner plexiform layer (IPL) gave 'on-centre' responses to luminance, and those that stratified in the outer IPL gave 'off-centre' responses. Phasic parasol cells gave no modulated responses to isoluminant chromatic stimuli optimized to reveal input from S-cones, consistent with previous conclusions that these cells receive little or no S-cone input¹³. Figure 1 shows responses of an on-centre phasic cell. Although the cell responded strongly to luminance modulation (Fig. 1a), there was no response to blue-yellow chromatic flicker (Fig. 1b) or to a stimulus modulated along a tritanopic confusion line (Fig. 1c), a condition in which only S-cones are modulated. Recordings from morphologically identified midget ganglion cells¹⁴ in the retinal periphery revealed, as expected, responses to both luminance modulation and red-green chromatic modulation⁴. However, like the parasol cells, these midget ganglion cells ($n=18$) showed no evidence of input from S-cones. Figure 1d-f illustrates the response of a green-on, red-off colour opponent cell identified as an inner midget ganglion cell. This

cell showed a clear opponent response to red and green set at equal luminance and modulated 180° out of phase (Fig. 1e). S-cone isolating stimuli (Fig. 1f) did not elicit a response.

Given the paucity of S-cones in the retina, it is conceivable that S-cone signals are transmitted to the LGN by only a small percentage of midget cells and our sample could have been too small to discover them. An alternative possibility is that a third ganglion cell type could convey S-cone signals to the LGN. We tested this by targeting a recently identified primate ganglion cell type, the small bistratified cell, whose axon projects to the parvocellular geniculate layers¹⁵. We were able to target the small bistratified cell for intracellular injection and recording *in vitro* by its characteristic cell body size and spatial density¹⁶.

All small bistratified cells recorded ($n=23$) received strong excitatory input from S-cones and resembled the blue-on cell that has been described physiologically¹⁷. All small bistratified cells gave a strong response to the S-cone isolating stimulus (Fig. 2), such that membrane depolarization and associated action potentials were always in phase with the S-cone modulation. The small bistratified cells also gave a sustained on-response to blue luminance modulation (Fig. 3a) and a clear off-response to yellow luminance modulation; isoluminant blue-yellow modulation elicited a strong blue-on response. Although it has been suggested that more than one cell class may receive excitatory S-cone input (F. M. De Monasterio and A. Mariani, personal communication), among the various non-midget, non-parasol ganglion cell types from which we have recorded, only the small bistratified cells have shown evidence of excitatory input from S-cones. In particular, we have found no cells that have both parasol-like morphology⁷ and excitatory S-cone input.

The distinctive morphology of the small bistratified cell suggests a specific neural circuitry that may give rise to blue-yellow colour opponency. The larger, inner dendritic field stratifies at precisely the same depth as the axon terminals of the blue-cone bipolar cells^{2,16}, making it likely that the blue-cone bipolar cell and the small bistratified cells form a synaptic pathway for excitatory S-cone signals in the retina. It seems probable that a second, hyperpolarizing bipolar cell type conveys M- and L-cone input directly to the outer dendritic tree. This arrangement would be consistent with the strong off-response to yellow luminance modulation shown in Fig. 3b and with the receptive field

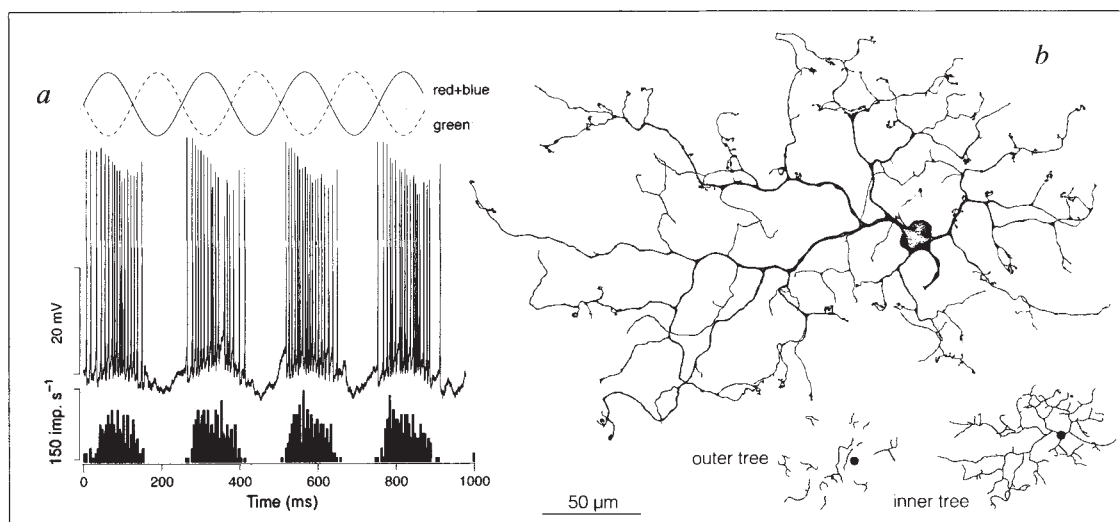


FIG. 2 Physiological and morphological identification of the blue-on ganglion cell type. *a*, The small bistratified cell gave a vigorous and sustained on-response to the same S-cone isolating stimulus that elicited null responses from the red-green opponent and phasic non-opponent cells shown in Fig. 1. Stimulus presentation at 4 Hz; all conventions as in Fig. 1. *b*, Dendritic morphology of cell whose intracellular

recording is shown in a displayed the pattern of bistratification and morphological features of all small bistratified cells¹⁶. The two tiers of the dendritic tree are traced separately (shaded insets) and illustrate that the inner tree forms a larger, more densely branched field than the outer dendrites.

FIG. 3 Small bistratified cells also gave characteristic blue-on, yellow-off responses. *a*, Intracellular recording of response to 4 Hz luminance modulation of blue LED. The cell showed a sustained on-response with hyperpolarization of membrane potential to luminance decrement. *b*, Off-response of the same cell to luminance modulation of a yellow light (red and green LEDs modulated in phase). The cell was hyperpolarized by a yellow luminance increment and gave a burst of spikes with luminance decrement. *c*, Response of the same cell to blue–yellow isoluminant chromatic modulation. Blue LED sine wave (solid line) is 180° out of phase with the in-phase modulation of the red and green LEDs (dotted line). *d*, Dendritic morphology of the small bistratified ganglion cell whose light response is shown in *a*, *b* and *c*. This cell was located at a lesser retinal eccentricity than the cell shown in Fig. 2 and consequently had a smaller overall dendritic field size¹⁶.

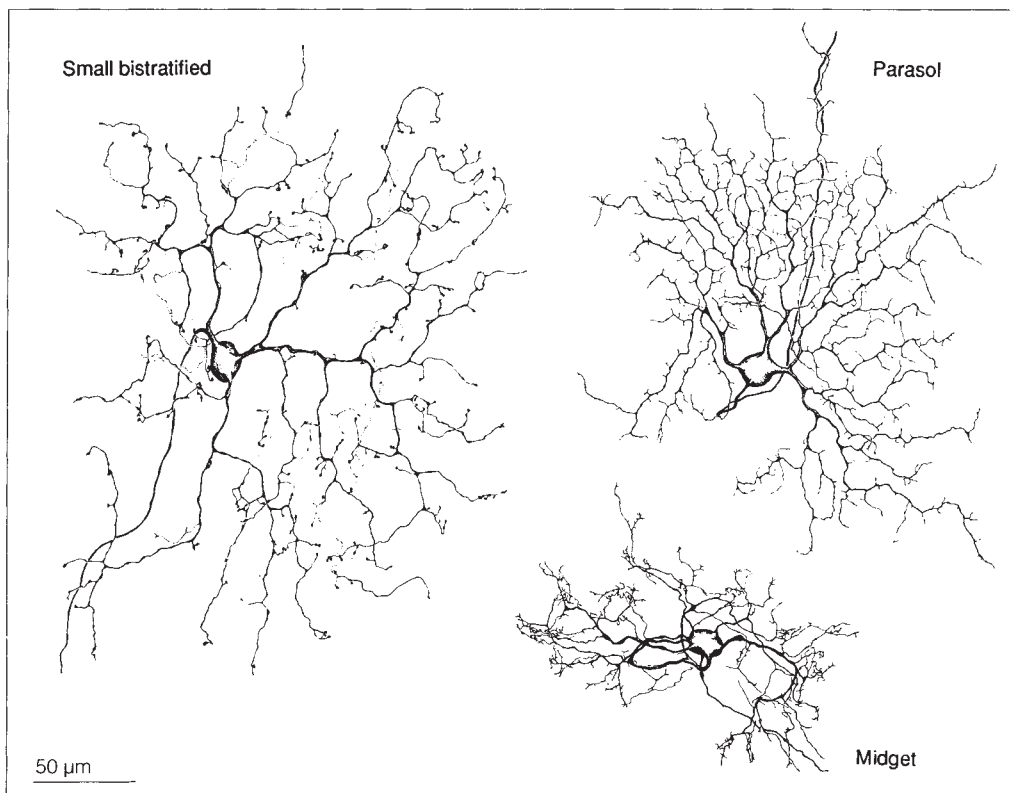
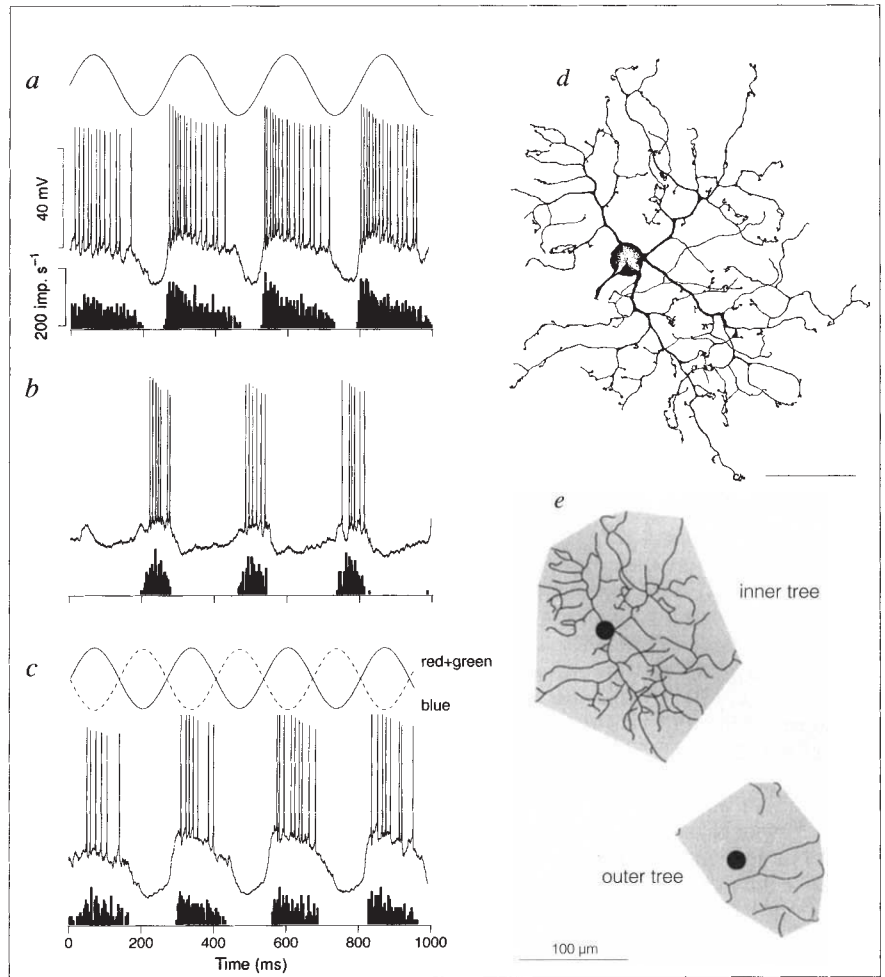


FIG. 4 Camera lucida tracings comparing the dendritic morphology of macaque ganglion cell types from the retinal periphery whose axons project to the dorsal lateral geniculate nucleus. The parasol cells give phasic, non-opponent on- or off-centre responses and project to the magnocellular LGN. The midget ganglion cells give red–green on- or off-centre opponent responses and project to the parvocellular LGN. The small bistratified ganglion cells give blue–yellow opponent responses of the blue-on type and also project to the parvocellular LGN. The blue-on, small bistratified ganglion cells have a dendritic field size similar to that of the non-opponent parasol cells, but differ from the parasol cells in the detailed shape of the dendritic tree.

structure of most blue-on cells, which are organized into spatially coextensive on and off regions^{18,19}.

Our results demonstrate an anatomical dichotomy in the primate parvocellular pathway which corresponds to the physiological dichotomy between the M, L- and S-cone systems. Midget ganglion cells convey M, L-cone opponent signals and the small bistratified cells convey S-cone excitatory signals (Fig. 4). It is not known whether there are other parallel pathways to the parvocellular layers. A blue-off cell type has been described^{18,20} and the possibility that ganglion cell types other than the midget cells convey M, L-cone opponent signals has been suggested¹⁶, but we have not encountered such cells.

Most mammals possess an S-cone system, but the existence of distinct M and L cones, and their use for trichromatic vision, seems to be a relatively recent evolutionary event²¹ which reflects a specialized adaptation in certain primates^{22,23}. The identification of separate ganglion cell types devoted to S-cone and M, L-cone signals is consistent with this picture of the evolution of primate colour vision. Moreover, our result supports a previous suggestion that the blue-on pathway may be kept anatomically segregated at the level of the LGN²⁴ and primary visual cortex²⁵, but its significance for further understanding the central pathways for colour-coding in primates remains largely to be explored. □

Received 6 September; accepted 24 November 1993.

- Mariani, A. P. *Nature* **308**, 184–186 (1984).
- Kouyama, N. & Marshak, D. W. *J. Neurosci.* **3**, 1233–1252 (1992).
- Boycott, B. B. & Wässle, H. *Eur. J. Neurosci.* **3**, 1069–1088 (1991).
- Reid, R. C. & Shapley, R. M. *Nature* **356**, 716–718 (1992).
- Leventhal, A. G., Rodieck, R. W. & Dreher, B. *Science* **213**, 1139–1142 (1981).
- Perry, V. H., Oehler, R. & Cowey, A. *Neuroscience* **12**, 1101–1123 (1984).
- De Monasterio, F. M. *Brain Res.* **166**, 39–48 (1979).
- Zrenner, E., Nelson, R. & Mariani, A. *Brain Res.* **262**, 181–185 (1983).
- Dacheux, R. F. & Raviola, E. *Proc. R. Soc. B* **239**, 213–230 (1990).
- Dacey, D. M. *Science* **240**, 1196–1198 (1988).
- Swanson, W. H., Ueno, T., Smith, V. C. & Pokorny, J. *J. opt. Soc. Am.* **A4**, 1992–2005 (1987).
- Famiglietti, E. V. Jr & Kolb, H. *Science* **194**, 193–195 (1976).
- Lee, B. B., Martin, P. R. & Valberg, A. *J. Physiol., Lond.* **404**, 323–347 (1988).
- Dacey, D. M. *J. Neurosci.* **13**, 5334–5355 (1993).
- Rodieck, R. W. in *From Pigments to Perception* (eds Valberg, A. & Lee, B. B.) 83–94 (Plenum, New York, 1991).
- Dacey, D. M. *Vis. Neurosci.* **10**, 1081–1098 (1993).

- Zrenner, E. & Gouras, P. *Vision Res.* **21**, 1605–1609 (1981).
- De Monasterio, F. M. & Gouras, P. *J. Physiol., Lond.* **251**, 167–195 (1975).
- Wiesel, T. N. & Hubel, D. H. *J. Neurophysiol.* **29**, 1115–1156 (1966).
- Valberg, A., Lee, B. B. & Tigwell, D. A. *Vision Res.* **26**, 1061–1064 (1986).
- Nathans, J., Thomas, D. & Hogness, D. S. *Science* **232**, 193–202 (1986).
- Mollon, J. D. *J. exp. Biol.* **146**, 21–38 (1989).
- Mollon, J. D., Estevez, O. & Cavonius, C. R. in *Vision: Coding and Efficiency* (ed. Blakemore, C.) 119–131 (Cambridge Univ. Press, UK, 1990).
- Schiller, P. H. & Malpeli, J. G. *J. Neurophysiol.* **41**, 788–797 (1978).
- Ts'o, T. & Gilbert, C. J. *J. Neurosci.* **8**, 1712–1727 (1988).
- Wyszecki, G. & Stiles, W. S. *Color Science: Concepts and Methods, Quantitative Data and Formulae* (Wiley, New York, 1982).
- Smith, V. C. & Pokorny, J. *Vis. Res.* **15**, 161–171 (1975).
- Dacey, D. M. & Brace, S. *Vis. Neurosci.* **9**, 279–290 (1992).

ACKNOWLEDGEMENTS. We thank J. Pokorny and V. Smith for help in setting up the LED stimulator, S. Buck for help with light calibration, and B. Boycott, C. Curcio, K. Mulligan, H. Sherk and J. Troy for their comments.

Dynamics of synaptic vesicle fusion and membrane retrieval in synaptic terminals

Henrique von Gersdorff & Gary Matthews

Department of Neurobiology and Behavior,
State University of New York, Stony Brook,
New York 11794–5230, USA

COMMUNICATION among neurons occurs at specialized synaptic junctions, where neurotransmitter is released via calcium-dependent exocytosis from the synaptic terminal of the presynaptic cell onto the postsynaptic target neuron. Here we exploit the unique properties of giant synaptic terminals^{1–4} of bipolar neurons from goldfish retina to establish the kinetics and calcium-dependence of exocytosis, and the characteristics of membrane retrieval following secretion in presynaptic terminals. Simultaneous patch-clamp, calcium-indicator dye and time-resolved capacitance measurements reveal that activation of calcium current drives secretion at a rapid rate of about 10,000 vesicles per s and the calcium level necessary to drive secretion is locally greater than 50 μM . Two components of membrane retrieval were observed following secretory stimulation. After strong stimulation, capacitance returned to rest with a time constant of about 30 s, but after weaker stimuli recovery was much faster, with a time constant of about 2 s. Secretion in a vertebrate central nervous system neuron was thus found to differ substantially from that in other secretory cells in its rapid rate of vesicle fusion, requirement for high levels of intracellular calcium, and the high speed and completeness of membrane retrieval. These distinctive features reflect the specialization of neuronal synaptic terminals for rapid and focally directed release of neurotransmitter.

Giant synaptic terminals of goldfish (*Carassius auratus*) retinal bipolar neurons are about 10 μm in diameter (Fig. 1a) and contain approximately 60 ribbon-type output sites⁵, each with

many small clear-core vesicles (~50 nm in diameter) tethered to the ribbon. Although the vesicles are small, the summed increase in membrane area at all of the output sites during secretion is sufficient to produce a detectable increase in capacitance (Fig. 1b). Activation of Ca^{2+} current (see inset, Fig. 1b) elicited an increase in intracellular calcium concentration ($[\text{Ca}^{2+}]_i$), accompanied by a rapid increase in capacitance, which returned to baseline within a few seconds. The capacitance response can be readily interpreted in terms of the dynamics of synaptic vesicle release and recycling. The rapid jump in capacitance in response to depolarization corresponds to the fusion (exocytosis) of a readily releasable pool of vesicles, such as those tethered to synaptic ribbons at release sites. The restoration of capacitance to resting level corresponds to membrane retrieval (endocytosis) and vesicle recycling^{6,7}. The amplitude of the jump in capacitance after a single 250-ms depolarization averaged 154 ± 36 fF ($n=27$), corresponding to the fusion of ~2,000 vesicles, or ~30 vesicles at each of the ~60 ribbon-type output sites.

To determine the rate of vesicle fusion, the duration of depolarization was varied (Fig. 2a). For pulse durations up to 180 ms, the capacitance response increased linearly with pulse duration at a rate of 730 fF s^{-1} , or ~10,000 vesicles s^{-1} . This rapidly releasable pool of vesicles was limited in size, however, because increasing the pulse duration beyond 180 ms caused no further increase in the capacitance jump. Figure 2b shows the dependence of the capacitance jump on the amplitude of depolarization. At voltages more negative than -20 mV, there was little change in capacitance, although Ca^{2+} current and increases in $[\text{Ca}^{2+}]_i$ were observed in this range of membrane potential (Fig. 2c). With further depolarization, Ca^{2+} current and the capacitance response increased, reaching a peak at 0 mV. At more positive membrane voltages, the capacitance response declined progressively until no change could be detected at potentials more positive than +50 mV. A similar relationship was observed for $[\text{Ca}^{2+}]_i$ (Fig. 2c), which suggests that the capacitance change was due to Ca^{2+} -dependent exocytosis.

To examine the calcium dependence of the capacitance response, exogenous calcium buffers (BAPTA and EGTA) were